Ultrasound in Med. & Biol., Vol. 33, No. 7, pp. 1132–1139, 2007

0301-5629/07/$–see front matter

ELSEVIER

doi:10.1016/j.ultrasmedbio.2007.01.005

● *Original Contribution*

ENHANCED TARGETING OF ULTRASOUND CONTRAST AGENTS USING ACOUSTIC RADIATION FORCE

JOSHUA J. RYCHAK,* ALEXANDER L. KLIBANOV,† KLAUS F. LEY,*‡ and JOHN A. HOSSACK‡
*University of Virginia Cardiovascular Research Center, Charlottesville, VA, USA; †University of Virginia Department of Internal Medicine, Charlottesville, VA, USA; and ‡University of Virginia Department of Biomedical Engineering, Charlottesville, VA, USA

(*Received* 19 *June* 2006; *revised* 18 *December* 2006; *in final form* 2 *January* 2007)

Abstract—Contrast-enhanced ultrasound has shown significant promise as a molecular imaging modality. However, one potential drawback is the difficulty that ultrasound contrast agents (UCA) may have in achieving adhesion to target molecules on the vascular endothelium. Microbubble UCA exhibit a lateral migration toward the vessel axis in laminar flow, preventing UCA contact with the endothelium. In the current study, we have investigated low-amplitude acoustic radiation as a mechanism to move circulating UCA toward targeted endothelium. Intravital microscopy was used to assess the retention of microbubble UCA targeted to P-selectin in the mouse cremaster microcirculation and femoral vessels. Acoustic treatment enhanced UCA retention to P-selectin four-fold in cremaster venules and in the femoral vein and 20-fold in the femoral artery. These results suggest acoustic treatment as a mechanism for enabling ultrasound-based molecular imaging in blood vessels with hemodynamic and anatomical conditions otherwise adversarial for UCA retention. (E-mail: jh7fj@virginia.edu) **© 2007 Published by Elsevier Inc. on behalf of the World Federation for Ultrasound in Medicine & Biology.**

Key Words: **Acoustic radiation force, Microbubble, Ultrasound imaging, Contrast enhanced ultrasound.**

INTRODUCTION

Targeted ultrasound contrast agents (UCA) have demonstrated utility for ultrasound-based molecular imaging. In a typical setting, the outer surface of a contrast agent is coated with a ligand that binds one or more target molecules of interest. Detection of agents accumulated at the target site using contrast-specific diagnostic ultrasound enables imaging of the targeted molecular event. This method has been used to image a number of physiological processes in animal models, including postischemic injury (Lindner et al. 2001), thrombus (Lanza et al. 1997; Hamilton et al. 2002; Schumann et al. 2002), tumor angiogenesis (Ellegala et al. 2003; Weller et al. 2005) and vascular remodeling in skeletal muscle (Leong-Poi et al. 2005).

Gas-encapsulated microbubbles are frequently used as targeted ultrasound contrast agents. The microbubble contrast agent was initially conceived as freely circulating blood tracer. The microvascular rheology of several nontargeted microbubble preparations has been shown to be very similar to that of erythrocytes (Ismail et al. 1996; Jayaweera et al. 1994; Lindner et al. 2002) and microscopic observations have confirmed that microbubbles tend to distribute toward the axis of the vessel (Keller et al. 1989). This characteristic enables the use of these agents as blood flow tracers for measuring vascular perfusion. However, for the purpose of molecular imaging, which requires that a circulating UCA come into contact with the targeted molecule at the vascular endothelium, lateral migration of an UCA toward the vessel axis is detrimental. In the microcirculation, hemodynamic and anatomical factors, such as postcapillary margination (Schmid-Schonbein et al. 1980), may facilitate UCA contact with the endothelium; however, such forces are largely absent in large blood vessels, especially in the arterial circulation. Thus, the frequent absence of UCA contact with the target surface may be a significant impediment to the widespread use of these agents for molecular imaging. This is especially pertinent for pathophysiology found in large vessels, such as thrombosis or atherosclerosis.

Address correspondence to: John A. Hossack, PhD, Department of Biomedical Engineering, MR5, 415 Lane Road, University of Virginia, PO Box 800759, Charlottesville, VA 22908-0759, USA. E-mail: jh7fj@virginia.edu

The application of low-intensity acoustic energy has been hypothesized as a mechanism to move freely flowing UCA toward the endothelium (Fowlkes et al. 1993; Dayton et al. 1997). The acoustic radiation force (also known as the Bjerkness force) consists of two components: these are a primary force directed away from the acoustic source and a secondary force, which is typically attractive between UCA. Dayton and colleagues verified that the primary radiation force was able to displace nontargeted UCA away from the vessel center in a flow chamber (Dayton et al. 1997, 1999a) and in the mouse microcirculation (Dayton et al. 1999b). The use of acoustic radiation force to enhance UCA adhesion to a target surface was subsequently examined *in vitro* (Rychak et al. 2005; Zhao et al. 2004). It was found that the retention of UCA targeted to the inflammatory protein P-selectin was increased significantly (up to 80-fold) by the application of acoustic radiation force and that this retention was specific. Significant clustering of UCA was observed after the application of acoustic radiation (Rychak et al. 2005), with up to 80% of the adherent UCA occurring in multiparticle aggregates. Acoustic radiation force has also been suggested as a mechanism to enhance the delivery of therapeutic substances (Lum et al. 2006; Shortencarier et al. 2004). In the current study, we examine the ability of applied acoustic radiation force to enhance the adhesion of UCA targeted to the inflammatory endothelial protein P-selectin *in vivo*. Contrast agent retention was examined in a model of inflammation in the mouse cremaster microcirculation and in the femoral artery and vein.

MATERIALS AND METHODS

Ultrasound contrast agents

The microbubble UCA used in this study were composed of decafluorobutane encapsulated by a lipid monolayer. The preparation of these agents has been described in depth elsewhere (Klibanov et al. 1999). The fluorescent probe DiI (Molecular Probes, Eugene, OR, USA) was incorporated into the lipid shell to enable microscopic detection of the agents.

The anti-P-selectin monoclonal antibody Rb40.34 (Bosse and Vestweber, 1994), prepared from hybridoma supernatant at the University of Virginia Lymphocyte Culture Center (Charlottesville, VA, USA), and an isotype-matched control (clone R3-34; BD Biosciences, San Jose, CA, USA) were used as targeting ligands. Targeting ligands were attached to the microbubble by means of biotin-streptavidin chemistry, as in Lindner et al. (2001). The size distribution and concentration of microbubble dispersions was characterized by electrozone sensing using a Coulter Multisizer IIe (Beckman-Coulter, Miami, FL, USA).

Animal preparation

Ten male C57/Bl-6 mice (Hilltop Labs, Scottsdale, PA, USA) and four male P-selectin knockout mice (derived from the colony described by Bullard et al. 1995) were used to examine UCA retention in the cremaster muscle microcirculation. Six mice in which the gene for green fluorescent protein had been knocked-in to the Lys-M locus (Faust et al. 2000) were used to examine UCA retention in the femoral vessels. All mice were housed at the University of Virginia animal facility and experiments were performed according to institutional guidelines.

Anesthesia was induced by an IP injection of 125 mg/kg body weight ketamine (Parke-Davis, Morris Plains, NJ, USA), 12.5 mg/kg xylazine (Phoenix Scientific, St. Joseph, MO, USA) and 0.025 mg/kg atropine sulfate (Elkins-Sinn, Cherry Hill, NJ, USA). Body temperature was maintained with a heat pad. Contrast agents were administered through a cannula made of PE-20 tubing (Becton Dickenson, Sparks, MD, USA) inserted into the right jugular vein and secured with sutures.

Intravital microscopy

P-selectin expression in the cremaster microcirculation was induced by the surgical trauma of exteriorizing the muscle (Ley et al. 1995). After preparation, the cremaster muscle was pinned to the stage of a custom-fabricated bath mounted to a compound videomicroscope (Carl Zeiss, Thornwood, NY, USA). The bath was filled to a depth of 50 mm with superfusion solution (131.9 mM NaCl, 18 mM $NaHCO_3$, 4.7 mM KCL, 2.0 mM $CaCl_2$*$2H_2O$, 1.2 mM $MgCl_2$ equilibrated with 5% CO_2) that was continuously circulated through a heater to maintain a constant temperature of 38°C. The ultrasound transducer was bolted to the stage at the focal distance (20.3 mm) from the cremaster using a ring stand and transmission of ultrasound energy occurred through the bath (Fig. 1). A bolus of 10^7 targeted or control UCA in

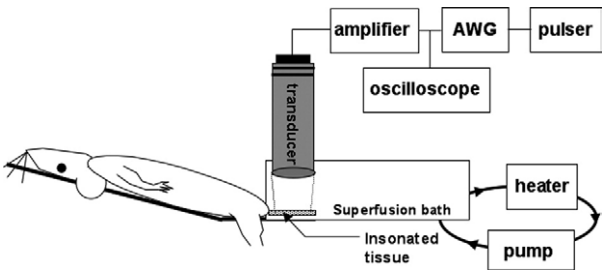

Fig. 1. Schematic of experimental apparatus. Acoustic energy was applied to the insonated tissue (femoral vessels or cremaster muscle) with a single element ultrasound transducer. The insonated tissue was immersed in a heated superfusion bath and the transducer was acoustically coupled to the tissue via the superfusion fluid.

~100 μL of saline was injected through the jugular cannula, followed by a 20 μL saline flush. Acoustic energy was applied to the cremaster tissue of 10 mice for 4 min immediately after administration of UCA. In four mice, no acoustic treatment was applied.

Contrast agent retention was assessed by fluorescence microscopy 4 min after UCA administration using a 40× immersion objective (40/0.8; Zeiss, Thornwood, NY, USA) and a high-resolution CCD camera (Dage-MTI, Michigan City, IN, USA). Contrast agents were illuminated using a filter set specific for DiI (λ_{ex} = 549 nm and λ_{em} = 565 nm); the preparation was subsequently transilluminated to observe the vasculature. The center line velocity (V_c) of each vessel was measured using a dual-slit photodiode (CircuSoft Instrumentation, Hockessin, DE, USA). The mean wall shear rate (γ_w) in each vessel was computed from the measured center line velocity (Lipowsky and Zweifach, 1978):

$$\gamma_w = 2.12[5 \cdot V_c/D] \quad (1)$$

where D is the diameter of the vessel (mm) and 2.12 is an empirical correction factor. Systemic leukocyte counts were determined from blood samples taken at the end of the experiment. A 10 μL blood sample was mixed with 90 μL Kimura to stain leukocytes. Leukocyte rolling flux fraction was computed from the number of rolling leukocytes observed per minute in each vessel ($N_{rolling}$), the mean vessel diameter (D), the mean blood velocity (V_b) and the systemic leukocyte count (C_{WBC}), as in Ley et al. (1995).

$$RFF = [N_{rolling}]/[0.25 \cdot \pi \cdot D^2 \cdot V_b \cdot 60 \cdot C_{WBC}] \quad (2)$$

Inflammation in the femoral vessels was induced by injection of 500 ng murine TNF-α (Sigma, St. Louis, MO, USA) into the plantar surface (Eriksson et al. 2001) of the left hind paw 3 h before UCA injection. The left leg was extended and secured with tape in a 10 cm × 5 cm × 10 cm deep bath on the operating stage and the skin on the posterior side of the leg was pinned aside to expose the femoral vessels. The bath was filled with circulated heated superfusion solution. A water-filled stand-off was used to maintain the ultrasound transducer at the focal distance (20.3 mm) from the tissue.

In the femoral vessel study, a bolus of 5×10^6 UCA was injected through the jugular cannula. This dosage was lower than that used for cremaster muscle to account for the higher blood flow through the femoral artery. The inflamed hindlegs of three Lys-GFP mice were insonated for 5 min immediately after UCA injection and three mice were not insonated. Retained UCA were observed by fluorescence microscopy on the posterior intravascular surface using a 20× immersion objective (Zeiss, SW 20/0.5) and filters specific for DiI 5 min after injection. The preparation was subsequently examined using a filter set specific for GFP (λ_{ex} = 498 nm and λ_{em} = 516 nm), which allowed visualization of the vessel walls and adherent leukocytes. No signal bleed was observed between fluorescence channels. A SIT camera (SIT 66, Dage-MTI) was used to observe the preparation, and videomicroscopic data were recorded onto a standard VHS cassette. Videomicroscopic images were digitized using Apple iMovie (v 5.0.2). The intravascular area of the posterior vessel surface was measured off-line and the number of leukocytes adherent within this area was determined.

Acoustic treatment

Ultrasonic acoustic energy was produced by a single-element transducer (Panametrics V306, Waltham, MA, USA) with a center frequency of 2.25 MHz, element diameter of 12.7 mm and spherical focal depth of 20.3 mm. A square-wave pulser (Ritec SP-801, Warwick, RI, USA) operating at a pulse repetition frequency of 10 kHz provided the trigger for an arbitrary waveform generator (Tektronix AWG 2021, Beaverton, OR, USA). The AWG output signal was amplified 50 dB by an RF power amplifier (ENI 325LA, Rochester, NY, USA) and the resulting sinusoidal waveform was monitored on an oscilloscope (Tektronix 2235). Forty sinusoidal cycles at a frequency of 2.0 MHz were applied to the tissue at an acoustic pressure of 50 kPa, determined with a needle hydrophone (Onda GL-0085, Sunnyvale, CA, USA). These acoustic parameters previously resulted in appreciable microbubble translation in an *in vitro* flow chamber system (Rychak et al. 2005) and were selected to induce appreciable microbubble translation while minimizing the possibility of microbubble destruction.

Analysis

Contrast agent retention was assessed after cessation of ultrasound in acoustically treated vessels. The number of retained UCA in the cremaster microcirculation was determined in 10 to 20 venules between 8 to 50 μm in diameter in each mouse. Only UCA that appeared intact and spherical were counted. In the femoral vessels, the number of retained UCA was determined in 8 to 12 contiguous fields-of-view at the upper thigh in the femoral artery and in the femoral vein. Each vessel was visualized on the posterior wall of the vessel (opposite the placement of the transducer). Contrast agent aggregation in the cremaster microcirculation was defined as two or more UCA adherent within one half UCA diameter (1.5 μm) of each other. Data in the cremaster are presented as mean retained UCA per venule ± standard deviation and as mean retained UCA per mm^2 posterior intravascular surface area in the femoral vessels. Statistical significance was determined with

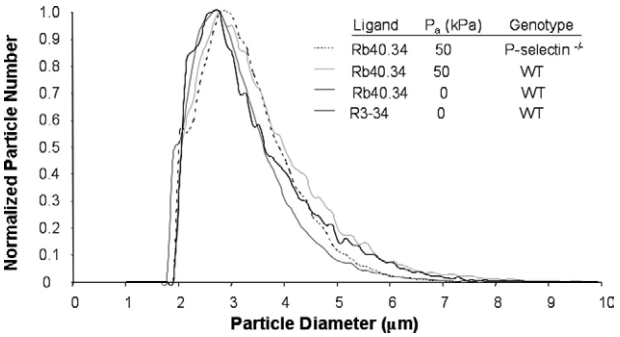

Fig. 2. Size distribution of ultrasound contrast agents used in these experiments. Electrozone analysis was used to determine UCA size characteristics.

one-way ANOVA using the Bonferroni adjustment for multiple comparisons, as appropriate, or the Student's *t*-test. Data were considered significant at $p < 0.05$.

RESULTS

The median particle diameter of all dispersions prepared for this study was between 3.3 and 3.8 μm (Fig. 2). No significant difference in median particle diameter between the preparations was detected using ANOVA. The size distributions of the particles exhibited a skewed normal distribution, with <0.5% of the particles being greater than 8.0 μm in diameter.

Hemodynamic properties of the venules examined in the cremaster microcirculation are summarized in Table 1. The mean venule diameter and wall shear rate were not significantly different between experimental groups. We inferred the presence of P-selectin from the leukocyte rolling flux fraction (RFF) and found no difference in mean RFF in all wild-type (WT) preparations. The RFF in P-selectin-deficient ($P^{-/-}$) mice was significantly lower than in the WT preparations, as would be expected from the dominant role of P-selectin in initiating leukocyte rolling in this model (Ley et al. 1995).

An approximately four-fold increase in UCA retention was observed after acoustic treatment relative to untreated preparations, shown in Fig. 3a. Retention appeared to be due to specific adhesion to P-selectin, as retention in $P^{-/-}$ mice and that of control-targeted UCA in WT mice were both negligible (Fig. 3a). Clustering of retained UCA was observed only for targeted UCA in WT mice treated with acoustic radiation, where approximately 25% of retention was in clusters of two or more UCA particles (Fig. 3b). Characteristic fields-of-view showing retained UCA in the cremaster microcirculation are given in Fig. 3c and d.

Expression of P-selectin in the femoral vessels was inferred from the presence of rolling leukocytes. A larger number of rolling leukocytes was observed in the femoral vein. A motion artifact due to respiration and pulse prevented accurate determination of the rolling flux fraction in this preparation, although the density of adherent leukocytes on the endothelial surface facing the microscope objective was measured from digitized in-focus frames. Leukocyte adhesion density was significantly greater in the femoral vein than artery in both acoustically-treated and untreated animals shown in Table 2. There was no detectable difference in leukocyte adhesion density due to application of acoustic radiation. The mean diameters of the femoral artery and vein segments were 188 ± 16 and 218 ± 11 μm, respectively. Intravascular area of the examined femoral vein and femoral artery segments were similar.

Ultrasound contrast agent retention on the intravascular surface facing the microscope objective of the femoral vessels was examined. An approximately four-fold increase in UCA retention after acoustic treatment was observed in the femoral vein, similar to that observed in the cremaster microcirculation. Virtually no UCA retention was observed in femoral artery segments that were not acoustically treated. We observed significant UCA retention in the acoustically-treated femoral artery, approximately 20-fold greater than that in the untreated condition (Fig. 4).

Table 1. Hemodynamic parameters in the cremaster microcirculation. Venule diameter and leukocyte rolling flux fraction (RFF) were measured from intravital videomicroscopic data. Wall shear rate was calculated from the measured center line velocity using 1

Genotype	Ligand	Acoustic pressure (kPa)	Venule diameter (μm)	Center line velocity (mm/s)	Wall shear rate (s^{-1})	RFF
WT	Rb40.34	0	21.7 ± 1.03	3.32 ± 0.30	1940 ± 368	14.7 ± 1.7
WT	Rb40.34	50	22.4 ± 5.54	2.77 ± 0.76	1837 ± 534	18.8 ± 16.4
WT	R3-34	50	25.5 ± 1.61	5.21 ± 0.58	2337 ± 140	19.3 ± 1.74
p-selectin$^{-/-}$	Rb40.34	50	26.6 ± 2.91	3.71 ± 1.15	1672 ± 675	0.385 ± 0.357†

All values expressed as mean ± standard deviation.
† $p < 0.05$ compared with other conditions.

Table 2. Vessel characteristic in the femoral vessels. Vessel area and RFF were computed from intravital microscopy data off-line. Mean posterior intravascular area per vessel segment and leukocyte adhesion density per vessel segment, ± standard deviation

Vessel	Acoustic pressure (kPa)	Intravascular area per segment (μm^2)	Adherent WBC/μm^2
Femoral artery	0	$6.9 \times 10^4 \pm 1.4 \times 10^4$	$10.8 \times 10^{-5} \pm 1.64 \times 10^{-5}$†
Femoral artery	50	$6.7 \times 10^4 \pm 0.2 \times 10^4$	$9.92 \times 10^{-5} \pm 1.67 \times 10^{-5}$‡
Femoral vein	0	$8.3 \times 10^4 \pm 0.3 \times 10^4$	$7.88 \times 10^{-4} \pm 0.48 \times 10^{-5}$
Femoral vein	50	$7.7 \times 10^4 \pm 0.7 \times 10^4$	$9.10 \times 10^{-4} \pm 2.81 \times 10^{-4}$

† $p < 0.05$ compared with femoral vein (0 kPa).
‡ $p < 0.05$ compared with femoral vein (50 kPa).

DISCUSSION

Ultrasound-based molecular imaging can offer significant utility at the clinical and preclinical levels. While the numerous advantages of this technique have been described elsewhere (Liang and Blomley, 2003; Lindner, 2004), a potential obstacle to efficient ultrasound-based molecular imaging is related to the size of the contrast agent. Other modalities, notably nuclear medicine, employ single-molecule contrast agents that are readily transported throughout the body. Contrast agents for ultrasound are necessarily particulate and subject to the shear forces imposed by blood flow. Lateral forces in laminar blood flow can inhibit microparticles (such as UCA) from crossing streamlines, resulting in axial colocalization with erythrocytes; this behavior is related to the size and compressibility of the particle (Nobis et al. 1985; Segre and Silberberg 1962) and has been confirmed for microbubbles *in vivo* (Keller et al. 1989) using intravital microscopy. Nonmicrobubble ultrasound contrast agents, such as acoustically-active liposomes and nanoparticle emulsions (Morowski et al. 2005), tend to be smaller than microbubbles and may therefore experience different lateral migratory forces. However, lateral forces that promote axial displacement may present a significant impediment to microbubble transport and adhesion to targeted endothelium.

A possible role for acoustic radiation in ultrasound-based molecular imaging and drug delivery has been

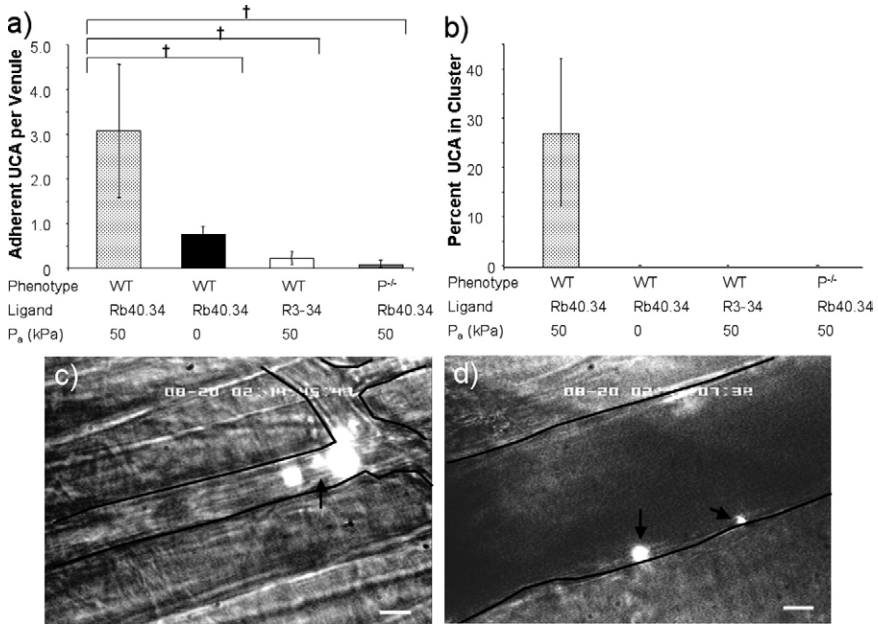

Fig. 3. Ultrasound contrast agent retention in venules of the cremaster microcirculation. Contrast agent retention was observed by intravital microscopy. (a) Mean number of retained UCA per venule ± standard deviation. (b) Fraction of retained UCA in aggregates of two or more, ± standard deviation. (c) and (d) Micrographs of P-selectin targeted UCA retained in two venules in WT mice after insonation. Vessel wall is outlined in black. Arrows indicate (c) adherent UCA aggregate and (d) single adherent UCA. Scale bar represents 10 μm. † $p < 0.05$.

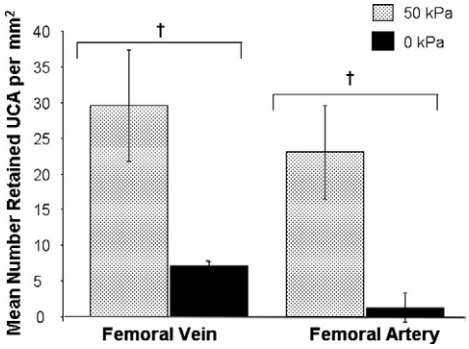

Fig. 4. Ultrasound contrast agent retention in the femoral vessels. Intravital microscopy was used to measure UCA retention in mouse femoral artery and vein segments. Density (number of retained UCA per mm^2) of UCA on the posterior intravascular surface of the femoral artery and vein. Data presented as mean ± standard deviation. † $p < 0.05$.

examined by several groups. Palanchon et al. (2005) have examined the ability of acoustic radiation force to displace air bubbles of various diameters, while Dayton et al. (1999a) reported similar results using UCA microbubbles. The ability of acoustic radiation force of various strengths to deflect and concentrate UCA has been characterized in an *in vitro* flow chamber system (Dayton et al. 1997, 1999b), and this effect has been shown to deflect nontargeted UCA away from the acoustic source *in vivo* (Dayton et al. 1999a). Acoustic radiation has been investigated as a mechanism to enhance targeted UCA retention to P-selectin (Rychak et al. 2005) and $\alpha_v\beta_3$-expressing cells (Zhao et al. 2004) *in vitro* using various flow chambers.

Previously, we (Rychak et al. 2005) observed that targeted UCA accumulation to a P-selectin-coated flow chamber surface decreased with increasing wall shear rate. Above ~700 s^{-1}, virtually no accumulation was observed. Acoustic treatment resulted in significant accumulation under the full range of wall shear rates examined (300 to 1200 s^{-1}). It is known that the axially directed lateral forces on a compressible particle are proportional to vessel shear rate, and we interpreted the *in vitro* results as evidence that the primary acoustic radiation force was able to counteract this tendency and induce UCA migration from the axis toward the target surface.

The *in vivo* results presented here suggest that vessel shear rate is not a robust predictor of the likelihood that an UCA contact the endothelium in all circumstances. Vessel shear rates in the microcirculation are significantly higher than in large vessels such as the femoral artery. Although we did not directly measure wall shear rates in the femoral vessels, we have used microparticle image velocimetry (Smith et al. 2003) to estimate center-line velocities on the order of 9 and 5 mm/s in TNF-α-treated mouse femoral artery and vein segments, respectively (data not shown and S. Unnikrishnan, unpublished results). Corresponding estimates for wall shear rates in the femoral artery and vein segments (approximately 500 and 250 s^{-1}, respectively) can be derived from the measured center-line velocities and vessel diameters. We observed appreciable UCA retention in the microcirculation without acoustic treatment, while retention in the femoral artery without acoustic treatment was virtually absent, despite a lower shear rate in this vessel. These data suggest that other factors, such as vascular anatomy, play a role in UCA retention. Margination of UCA at drainage points, which could force an UCA into contact with the endothelium, may account for the observed UCA retention in untreated venules and the femoral vein. A similar mechanism occurs in leukocyte adhesion to P-selectin (Eriksson et al. 2001; Schmid-Schonbein et al. 1980). In the femoral artery, there are no confluent bifurcations and anatomically-determined marginating forces are absent. Differences in P-selectin expression between the various vasculatures may also account for the observed differences in UCA retention.

Adhesion of an UCA to a molecular target requires that the target be expressed in density sufficient to support UCA retention and that the UCA comes into contact with the target. Thus, targeted contrast-enhanced ultrasound images represent not the total density of the molecular target in the imaged tissue, but rather the density of the molecular target in vessels in which hemodynamic conditions enable UCA contact with the endothelium. This limitation may confound interpretation of imaging data, although ultrasound contrast intensity has been shown to correlate well with histologic data for some microcirculatory molecular markers such as MAdCAM-1 (Bachmann et al. 2006). In particular, imaging molecular targets in vessels with adversarial hemodynamics and anatomy, specifically arteries, may present difficulty. We have shown that acoustic treatment can enhance specific UCA retention in vessels that enable hemodynamic UCA margination toward the endothelium (femoral vein and cremaster venules), as well as under adversarial hemodynamic conditions (femoral artery). This technique may serve to increase the range of vessels that a circulating UCA may sample, enabling a more robust mode of molecular imaging.

Our findings suggest one potential limitation of the use of acoustic treatment. We observed clustering of retained UCA within the microcirculation. Although we cannot determine whether acoustic treatment induces aggregation of circulating UCA or simply causes preferential retention in clusters, this is a factor that must be investigated thoroughly. Aggregation of circulating UCA may cause occlusion and the echogenicity of aggregated UCA may be significantly altered. Experiments by Day-

ton et al. (1999b) suggest that secondary radiation-force-induced aggregates remain echogenic, although the susceptibility of aggregates to acoustic destruction may be reduced. A reduction in the UCA dose and systemic concentration will decrease a chance of multiparticle aggregation, although aggregation may be beneficial for UCA used as drug delivery devices, as in Lum et al. (2006) and Shortencarier et al. (2004). The UCA dosages used in this study were similar to those typically used for contrast-enhanced ultrasound imaging in mice (Lindner et al. 2001). Additionally, we administered acoustic energy in an open preparation, which diminishes ultrasound attenuation from intervening tissue. It is clear that the acoustic parameters must be carefully calibrated to ensure optimal acoustic treatment in various tissues.

In summary, we have investigated the ability of acoustic radiation force to mediate targeted UCA adhesion to P-selectin. The exteriorized cremaster muscle was used as a model of UCA retention in the microcirculation. Appreciable targeted retention was observed in the absence of acoustic treatment, although UCA retention was significantly greater in insonated preparations. UCA aggregation was observed in insonated, but not in control, preparations. Cytokine-stimulated femoral vein and artery were used as models for UCA retention in large vessels. Acoustic treatment yielded a significant increase in UCA retention in both vessels. This effect was most pronounced in the femoral artery, where acoustic treatment greatly enhanced the negligible baseline retention.

Acknowledgments—This work was sponsored in part by NIH NIBIB EB001826 to J.H. J.R. was supported by Cardiovascular Training Grant HL07284 to University of Virginia. A portion of this work was presented at the 2005 IEEE Ultrasound, Ferroelectrics and Frequency Control Symposium. Technical assistance from Su Htay, Lavanya Peddada and Shiwei Zhao is gratefully acknowledged. The authors appreciate discussion regarding this work from Paul Dayton, Susannah Bloch and Mark Borden and are grateful for the assistance of Jonathan Lindner.

REFERENCES

Bachmann C, Klibanov AL, Olson TS, Sonnenshein JR, Rivera-Nieves J, Cominelli F, Ley KF, Lindner JR, Pizarro TT. Targeting mucosal address in cellular adhesion molecule (MAdCAM)-1 to noninvasively image experimental Crohn's disease. Gastroenterology 2006; 130:8–16.

Bosse R, Vestweber D. Only simultaneous blocking of the L- and P-selectin completely inhibits neutrophil migration into mouse peritoneum. Eur J Immunol 1994;24:3019–3024.

Bullard DC, Qin L, Lorenzo I, Quinlin WM, Doyle NA, Bosse R, Vestweber D, Doerschuk CM, Beaudet AL. P-selectin/ICAM-1 double mutant mice: Acute emigration of neutrophils into the peritoneum is completely absent but is normal in pulmonary alveoli. J Clin Invest 1995;95:1782–1788.

Dayton PA, Morgan KE, Klibanov AL, Brandenburger G, Nightingale KR, Ferrara KW. A preliminary evaluation of the effects of primary and secondary radiation forces on acoustic contrast agents. IEEE Trans. Ultrason Ferroelectr Freq Control 1997;44:1264–1277.

Dayton PA, Klibanov A, Brandenburger G, Ferrara K. Acoustic radiation force *in vivo*: A mechanism to assist targeting of microbubbles. Ultrasound Med Biol 1999a;25:1195–1201.

Dayton PA, Morgan KE, Klibanov A, Brandenburger G, Ferrara KW. Optical and acoustical observations of the effects of ultrasound on contrast agents. IEEE Trans Ultrasound Ferroelec Freq Control 1999b;46:220–232.

Ellegala DB, Leong-Poi H, Carpenter JE, Klibanov AL, Kaul S, Shaffrey ME, Sklenar J, Lindner JR. Imaging tumor angiogenesis with contrast ultrasound and microbubbles targeted to alpha(v) beta3. Circulation 2003;108:336–341.

Eriksson EE, Xie X, Werr J, Thoren P, Lindbom L. Importance of primary capture and L-selectin dependent secondary capture in leukocyte accumulation in inflammation and atherosclerosis *in vivo*. J Exp Med 2001;194:205–218.

Faust N, Varas F, Kelly LM, Heck S, Graf T. Insertion of enhanced green fluorescent protein into the lysozyme gene creates mice with green fluorescent granulocytes and macrophages. Blood 2000;96: 719–726.

Fowlkes JB, Gardner EA, Ivey JA, Carson PL. The role of acoustic radiation force in contrast enhancement techniques using bubble-based ultrasound contrast agents. J Acoust Soc Am 1993;93:2348.

Hamilton A, Huang SL, Warnick D, Stein A, Rabbat M, Madhav T, Kane B, Nagaraj A, Klegerman M, MacDonald R, McPherson D. Left ventricular thrombus enhancement after intravenous injection of echogenic immunoliposomes: Studies in a new experimental model. Circulation 2002;105:2772–2778.

Ismail S, Jayaweera AR, Camarano G, Gimple LW, Powers ER, Kaul S. Relation between air-filled albumin microbubble and red blood cell rheology in the human myocardium: Influence of echocardiographic systems and chest wall attenuation. Circulation 1996;94: 445–451.

Jayaweera AR, Edwards N, Glasheen WP, Villanueva FS, Abbot RD, Kaul S. *In vivo* myocardial kinetics of air filled albumin microbubbles during myocardial contrast echocardiography: Comparison with radiolabeled red blood cells. Circ Res 1994;74:1157–1165.

Keller MW, Segal SS, Kaul S, Duling BR. The behavior of sonicated albumin microbubbles within the microcirculation: A basis for their use during myocardial contrast echocardiography. Circ Res 1989; 65:458–467.

Klibanov AL, Gu H, Wojkyla JK, Wible JH, Kim DH, Needham D, Villanueva FS, Brandenburger GH. Attachment of ligands to gas-filled microbubbles via PEG spacer and lipid residues anchored at the interface. Proceedings of the International Symposium on Controlled Release of Bioactive Materials. Boston, MA: Controlled Release Society. 1999;26:124–125.

Lanza GM, Wallace KD, Fischer SE, Christy DH, Scott MJ, Trousil RL, Cacheris WP, Miller JG, Gaffney PJ, Wickline SA. High-frequency ultrasonic detection of thrombi with a targeted contrast system. Ultrasound Med Biol 1997;23:863–870.

Leong-Poi H, Swales J, Jayaweera AR, Bin JP, Kaul S, Lindner JR. Effect of microbubble exposure to ultrasound on quantitation of myocardial perfusion. Echocardiogr 2005;22:503–509.

Ley K, Bullard DC, Arbones ML, Bosse R, Vestweber D, Tedder TF, Beaudet AL. Sequential contribution of L- and P-selectin to leukocyte rolling *in vivo*. J Exp Med 1995;181:669–676.

Liang H-D, Blomley MJK. The role of ultrasound in molecular imaging. Br J Radiology 2003;76:140–150.

Lindner JR, Jayaweera AR, Sklenar J, Kaul S. Microvascular rheology of Definity microbubbles after intra-arterial and intravenous administration. J Am Soc Echocardiogr 2002;15:396–403.

Lindner JR, Song J, Christiansen J, Klibanov AL, Xu F, Ley K. Ultrasound assessment of inflammation and renal tissue injury with microbubbles targeted to P-selectin. Circulation 2001;104:2107–2112.

Lindner JR. Microbubbles in medical imaging: Current applications and future directions. Nat Rev Drug Discov 2004;3:527–532.

Lipowsky HH, Zweifach BW. Application of the "two-slit" photometric technique to the measurement of microvascular volumetric flow rates. Microvasc Res 1978;15:93–101.

Lum AF, Borden MA, Dayton PA, Kruse DE, Simon SI, Ferrara KW. Ultrasound radiation force enables targeted deposition of model drug carriers loaded on microbubbles. J Control Release 2006; 111:128–134.

Morawski AM, Lanza GA, Wickline SA. Targeted contrast agents for magnetic resonance imaging and ultrasound. Curr Opin Biotechnol 2005;16:89–92.

Nobis U, Pries AR, Cokelet GR, Gaehtgens P. Radial distribution of white cells during blood flow in small tubes. Microvasc Res 1985; 29:295–304.

Palanchon P, Tortoli P, Bouakaz A, Versluis M, de Jong N. Optical observations of acoustical radiation force effects on individual air bubbles IEEE Trans. Ultrasound Ferroelec Freq Control 2005;52: 104–110.

Rychak JJ, Klibanov AL, Hossack J. Acoustic radiation force enhances targeted delivery of ultrasound contrast microbubbles: *In vitro* verification IEEE Trans Ultrasound Ferroelec Freq Control 2005; 52:421–433.

Schmid-Schonbein GW, Skalak R, Usami S, Chien S. Cell distribution in capillary networks. Microvasc Res 1980;19:18–44.

Schumann PA, Christiansen JP, Quigley RM, McCreery TP, Sweitzer TH, Unger EC, Lindner JR, Matsunaga TO. Targeted-microbubble binding selectively to GPIIB IIIA receptors of platelet thrombi. Invest Radiol 2002;37:587–593.

Segre G, Silberberg A. Behavior of macroscopic rigid particles in Poiseulle flow II experimental results and interpretation. J Fluid Mech 1962;14:136–157.

Shortencarier MJ, Dayton PA, Bloch SH, Schumann PA, Matsunaga TO, Ferrara KW. A method for radiation-force localized drug delivery using gas-filled lipospheres. IEEE Trans Ultrason Ferroelectr Freq Control 2004;51:822–831.

Smith ML, Long DS, Damiano ER, Ley K. Near-wall micro-PIV reveals a hydrodynamically relevant endothelial surface layer in venules in vivo. Biophys J 2003;85:637–645.

Weller GER, Wong MKK, Modzelewski RA, Lu E, Klibanov AL, Wagner WR, Villanueva FS. Ultrasonic imaging of tumor angiogenesis using contrast microbubbles targeted via the tumor-binding peptide arginine-arginine-leucine. Cancer Res 2005;65:533–539.

Zhao S, Borden M, Bloch S, Kruse D, Ferrara KW, Dayton PA. Radiation force assisted targeting facilitates ultrasonic molecular imaging. Molecular Imaging 2004;3:1–14.